# Calcium signaling mediates mechanotransduction at the multicellular stage of *Dictyostelium discoideum*

Hidenori Hashimura[1,2,3,*], Yusuke V. Morimoto[2,4,5,*,‡], Yusei Hirayama[4] and Masahiro Ueda[1,2,6]

[1] Department of Biological Sciences, Graduate School of Science, Osaka University, 1-3 Yamadaoka, Suita, Osaka 565-0871, Japan.
[2] RIKEN Center for Biosystems Dynamics Research (BDR), 6-2-3 Furuedai, Suita, Osaka 565-0874, Japan.
[3] Graduate School of Arts and Sciences, University of Tokyo, 3-8-1 Komaba, Meguro, Tokyo 153-8902, Japan.
[4] Faculty of Computer Science and Systems Engineering, Kyushu Institute of Technology, 680-4 Kawazu, Iizuka, Fukuoka 820-8502, Japan.
[5] Japan Science and Technology Agency, PRESTO, 4-1-8 Honcho, Kawaguchi, Saitama, 332-0012, Japan
[6] Graduate School of Frontier Biosciences, Osaka University, 1-3 Yamadaoka, Suita, Osaka 565-0871, Japan.

* These authors contributed equally.

‡ Corresponding author: e-mail: yvm001@phys.kyutech.ac.jp

Running title: Mechanotransduction in *Dictyostelium* multicellular body

Keywords: mechanotransduction; calcium signaling; ion channel; multicellular system; *Dictyostelium*

## Summary statement

Fluorescence imaging revealed that calcium signaling via both endoplasmic reticulum and extracellular pathways plays an important role in mechanosensing during the multicellular stage of *Dictyostelium*.

## Abstract

Calcium acts as a second messenger and regulates cellular functions, including cell motility. In *Dictyostelium discoideum,* the cytosolic calcium level oscillates synchronously, and calcium signal waves propagate in the cell population during the early stages of development, including aggregation. At the unicellular phase, the calcium response through Piezo channels also functions in mechanosensing. However, calcium signaling dynamics during multicellular morphogenesis is still unclear. Here, live-imaging of cytosolic calcium levels revealed that calcium wave propagation, depending on cAMP relay, temporarily disappeared at the onset of multicellular body formation. Alternatively, the occasional burst of calcium signals and their propagation were observed in both anterior and posterior regions of migrating multicellular bodies. Calcium signaling in multicellular bodies occurred in response to mechanical stimulation. Both pathways, calcium release from the endoplasmic reticulum via IP3 receptor and calcium influx from outside the cell, were involved in calcium waves induced by mechanical stimuli. These show that calcium signaling works on mechanosensing in both the unicellular and multicellular phases of *Dictyostelium* using different molecular mechanisms during development.

## Introduction

$Ca^{2+}$ signals are essential for several types of biological activities (Clapham, 2007; Parekh, 2011). In multicellular organisms, the synchronized elevation of intracellular $Ca^{2+}$ levels ($[Ca^{2+}]_i$) occurs in cell populations, and this "$[Ca^{2+}]_i$ burst" propagates as waves among cells (Berridge et al., 2003; Leybaert and Sanderson, 2012). This phenomenon has been reported in various cell types and biological activities, such as fertilization in eggs and wound repair of endothelial cells (Chifflet et al., 2012; Whitaker, 2006). $[Ca^{2+}]_i$ burst and wave propagation play key roles in orchestrating multiple cells *in vivo* and *in vitro* (Parekh, 2011). Cell-cell communication via $Ca^{2+}$ signaling has been well investigated in animals, and it has revealed that $Ca^{2+}$ waves are propagated by gap junction communication, or paracrine signaling (Leybaert and Sanderson, 2012). A factor evoking the $[Ca^{2+}]_i$ burst is a mechanical stimulus, and transduction of mechanical stimuli into $Ca^{2+}$ signals is mediated by varied $Ca^{2+}$ channels such as inositol trisphosphate (IP3) receptors, transient receptor potential (TRP) channels, and the stretch-activated ion channel Piezo (Canales et al., 2019; Coste et al., 2010; Fang et al., 2021; Prole and Taylor, 2019; Volkers et al., 2015; Yin and Kuebler, 2010). These channels are broadly conserved in eukaryotes including animals, plants, and amoebae (Coste et al., 2010; Volkers et al., 2015; Yin and Kuebler, 2010). Hence, there is a possibility that $Ca^{2+}$ signaling is universally employed in various organisms for mechanosensing.

One example of $Ca^{2+}$ wave propagation among populations of eukaryotic cells is cell-cell communication in the aggregation of social amoebae, *Dictyostelium*

*discoideum*. Following starvation, *Dictyostelium* cells aggregate and form cell masses called mounds. Cells in a mound differentiate into either a prestalk or prespore cells and form migrating multicellular bodies called slugs. During aggregation, intercellular cAMP signaling, known as cAMP, relay organizes directed migration of cells (Gregor et al., 2010; Hashimura et al., 2019; Tomchik and Devreotes, 1981), and $Ca^{2+}$ waves are propagated simultaneously among starved cells (Horikawa et al., 2010). It has been assumed that cAMP relay is essential for the coordination of collective cell migration through *Dictyostelium* development (Singer et al., 2019; Weijer, 1999); however, recent studies have shown that the dynamics of cAMP signaling shows transition after multicellular formation (Fujimori et al., 2019; Hashimura et al., 2019). In addition to $Ca^{2+}$ wave propagation during aggregation (Horikawa et al., 2010), transient $[Ca^{2+}]_i$ elevation has been observed in mounds and slugs (Cubitt et al., 1995). These results suggest that $[Ca^{2+}]_i$ signaling such as synchronous $[Ca^{2+}]_i$ burst and wave propagation occurs not only during aggregation but also in the latter development stages of *Dictyostelium* cells, including mounds and slugs. However, the dynamics and molecular mechanisms of $[Ca^{2+}]_i$ signaling during the morphogenesis of *Dictyostelium* are still unclear.

In this study, the $[Ca^{2+}]_i$ signaling through the development of *Dictyostelium* cells was investigated. This approach revealed the transition of $[Ca^{2+}]_i$ signaling dynamics during the multicellular formation and the multicellular bodies of *Dictyostelium* have robust calcium signaling mechanisms in response to mechanical stimuli.

# Results

## Transition of calcium signaling dynamics in cell populations during the development of *Dictyostelium* cells

To investigate the relationship between the dynamics of calcium signals and multicellular formation in *Dictyostelium,* we monitored $[Ca^{2+}]_i$ dynamics during development with genetically-encoded calcium indicators (GECI). As previously reported (Horikawa et al., 2010), cells expressing the Förster resonance energy transfer (FRET) sensor YC-Nano15 (Kd = 15 nM) showed clear oscillations and wave propagation of fluorescence signals in aggregation streams (Fig. 1A, Fig. S1A, and Movie 1). Moreover, $[Ca^{2+}]_i$ dynamics was also investigated with the single-wavelength GECI, GCaMP6s (Chen et al., 2013; Pervin et al., 2018), to confirm whether the wave propagation of fluorescence signals of YC-Nano15 authentically reflected the $[Ca^{2+}]_i$ dynamics during development using the other GECI and avoiding the phototoxicity caused by exposure of violet-blue light excitation for YC-Nano15. In starved *Dictyostelium* cells, $[Ca^{2+}]_i$ transiently increases in response to external cAMP (Yumura et al., 1996) and the calcium channel IplA, which is the homologue of IP3 receptor, is essential for its elevation (Traynor et al., 2000). When chemotactic-competent cells expressing GCaMP6s were stimulated by cAMP, wild-type cells showed transient rapid elevation of fluorescence signals with a peak at 16 s after stimulation; however, cells lacking *iplA* show no increase of signals after stimuli (Fig S2A). Thus, GCaMP6s (Kd = 144 nM) (Chen et al., 2013) is functional in *Dictyostelium* cells and appropriate to visualize $[Ca^{2+}]_i$ dynamics during aggregation and sequential development. Oscillations of fluorescence signals and wave propagation were observed at the

early aggregation and mound stages of cells expressing GCaMP6s (Fig. 1B–D, Fig. S1B–D, Movies 2–6). These signal propagation and oscillations were not observed in the populations of *iplA*$^{-}$ cells during development (Fig. S2B, C, Movie 7), demonstrating that the periodic changes in GCaMP6s signals in developing *Dictyostelium* cells reflects $[Ca^{2+}]_i$ oscillations caused by cAMP signal relay. The period of oscillations at the early mound stage was significantly shorter than those at the early aggregation and late mound stages ($p < 0.001$) (Fig. 1E). The early and late mound stages observed in this study correspond to the loose and tight mound stages, respectively. The periods of $[Ca^{2+}]_i$ oscillations at the early aggregation, early and late mound stages were 5.29 ± 0.59, 2.95 ± 0.61, and 4.60 ± 0.89 min, respectively. These periods are consistent with those of $[cAMP]_i$ oscillations (Hashimura et al., 2019). Wave propagation was observed until the late mound stage; however, signal oscillations and propagation in cell populations disappeared when the late mound began elongation, which is the onset of multicellular slug formation (Fig. 1F–H, Movie 8). These indicate that $[Ca^{2+}]_i$ signal dynamics show transition during multicellular morphogenesis as well as cAMP signal dynamics (Hashimura et al., 2019).

**Transient $[Ca^{2+}]_i$ burst and its propagation in migrating slugs**

In the late stage of *Dictyostelium* development, the late mound elongates into a cylindrical structure called a finger, and finger subsequently falls over and starts to migrate as a slug. When monitoring $[Ca^{2+}]_i$ dynamics in migrating slugs using YC-Nano15, transient and rapid elevation of $[Ca^{2+}]_i$, namely "$[Ca^{2+}]_i$ burst" and its propagation was observed (Fig. 2A, B, Movie 9), although no wave propagation

148 was observed at the finger stage (Fig. 1). Monitoring the signal using GCaMP6s
149 also detected such transient signal propagation in migrating slugs, and the $[Ca^{2+}]_i$
150 bursts were observed in both the anterior and posterior part of slugs which can
151 be regarded as the prestalk and prespore region, respectively (Fig. 2C–F, Movies
152 10, 11). When the $[Ca^{2+}]_i$ burst occurred in the slug, the velocity of slug migration
153 transiently increased with a peak delay of approximately 2 min (Fig. 2B, Movie 9).
154 The periodicity of $[Ca^{2+}]_i$ signals as observed in cell populations during
155 aggregation and mound stages (Fig. 1) was not observed in migrating slugs, and
156 slugs occasionally showed irregular $[Ca^{2+}]_i$ burst (Fig. 2 and S3). Thus, although
157 periodic $[Ca^{2+}]_i$ signal propagations disappeared during the process of
158 multicellular formation, the ability of $Ca^{2+}$ signaling was maintained after slug
159 formation, and the occasional propagation of $[Ca^{2+}]_i$ waves in migrating slugs
160 affected the cooperative movement of cells.
161
162 **$[Ca^{2+}]_i$ burst and wave propagation in slugs are induced by mechanical**
163 **stimulation**
164 On closer observation, $[Ca^{2+}]_i$ burst in slugs occurred when a part of the slug
165 touched the surface of the agar (Fig. 2C, E and Movies 10, 11). This proposes
166 the possibility that rapid $[Ca^{2+}]_i$ elevation in slugs was induced in response to
167 mechanical stimuli. To confirm this, $[Ca^{2+}]_i$ dynamics was monitored using
168 GCaMP6s when the slug was subjected to mechanical stimulation. The slug
169 developed on the agar was cut out with the agar, turned over onto the glass,
170 sandwiched between the glass and the agar, and pressed from above with a 5
171 mm diameter plastic rod such that the slug was not crushed, and the entire slug

was stimulated evenly (Fig. S4A). In all tests using wild-type expressing GCaMP6s, $[Ca^{2+}]_i$ in the slug increased transiently with a peak at 25.0 ± 4.1 s after all stimulation (n = 9) (Fig. 3A, B and Movie 12). Additionally, when the tip of a slug was pricked using a micropipette (Fig. S4B), $[Ca^{2+}]_i$ burst was induced and signal waves were propagated toward the posterior region (Fig. 3C, D and Movie 13). A similar response was observed when the posterior region of the slug was stimulated (Fig. 3E, F and Movie 14). These indicate that $[Ca^{2+}]_i$ burst and wave propagation in the slug occurs in response to mechanical stimulation. In addition, this mechanical response can be applied to either the anterior or posterior regions of the slug.

**IplA $Ca^{2+}$ channel is involved in calcium signaling in response to mechanical stimulation in the slug**

At the unicellular phase of *Dictyostelium*, the IP3 receptor IplA, which is localized in the endoplasmic reticulum (ER), is involved in calcium signaling, and responsible for $[Ca^{2+}]_i$ elevation in response to mechanical stimuli (Lombardi et al., 2008). To confirm whether IplA is involved in $[Ca^{2+}]_i$ burst induced by mechanical stimulation in a slug, $[Ca^{2+}]_i$ signal responses to mechanical stimuli in slugs lacking *iplA* was investigated. When *iplA*$^-$ slugs were stimulated with a plastic rod, $[Ca^{2+}]_i$ bursts occurred; however, the percentage of slug that responded dropped to 46% (n = 39), and the response peaked at 15.7 ± 7.9 s (n = 18), earlier than in the wild type (Fig. 3, 4). Calcium response was also observed when *iplA*$^-$ slugs bumped into the agar as well as the wild type (Fig. S5). These results suggest that $[Ca^{2+}]_i$ burst and wave propagation in response to

196 mechanical stimuli are partially mediated by the IplA channel.

197

198 **Calcium influx from outside the cell allows for a rapid response to**
199 **mechanical stimuli**

200 Deletion of IplA did not completely abolish the calcium response of the slug to
201 mechanical stimulation (Fig. 4), indicating that another calcium pathway
202 contributes to mechanosensing. It has been reported that extracellular $Ca^{2+}$ influx
203 via the Piezo channel homolog is important for mechanosensing at the unicellular
204 stage of *Dictyostelium* (Srivastava et al., 2020). To investigate whether $Ca^{2+}$ influx
205 from outside the cell occurs even in the multicellular stage, calcium response was
206 monitored with the agar medium containing ethylene glycol-bis(β-aminoethyl
207 ether)-N,N,N′,N′-tetraacetic acid (EGTA), a $Ca^{2+}$ chelating agent. All multicellular
208 bodies overlayed with agar containing 1 mM EGTA showed an increase in $[Ca^{2+}]_i$
209 in response to mechanical stimuli (n = 13) (Fig. 5A, B). However, in the presence
210 of EGTA, the response peak was significantly slower at 67.7 ± 16.8 seconds ($p <$
211 0.001) (Fig. 5B, E). Additionally, *iplA*$^-$ slugs in the presence of 1 mM EGTA did not
212 show any calcium response to mechanical stimulation (n = 13) (Fig. 5C). These
213 and *iplA*$^-$ deficient results indicate that $Ca^{2+}$ influx from extracellular sources
214 allows a fast response, whereas IplA is essential for the response from
215 intracellular sources (Fig. 4, 5C). We constructed the PzoA null strain and
216 confirmed that PzoA is essential for $Ca^{2+}$ influx from extracellular sources by
217 mechanical stimulation in unicellular cells as previously reported (Fig. S6)
218 (Srivastava et al., 2020). In contrast, multicellular bodies of *pzoA*$^-$ strain
219 responded similarly to wild-type cells, suggesting that $Ca^{2+}$ influx occurs from

other pathways during the multicellular phase (Fig. 5D, E).

## Discussion

In *Dictyostelium* cells, transient $[Ca^{2+}]_i$ changes have been observed in the mound and slug stages (Cubitt et al., 1995); however, the actual dynamics of $Ca^{2+}$ signaling has not been clarified, because most previous studies of calcium signaling have focused on the stages up to cell aggregation (Horikawa et al., 2010; Nebl and Fisher, 1997; Schlatterer et al., 1992; Traynor et al., 2000). In this study, live imaging of $[Ca^{2+}]_i$ during the development of *Dictyostelium* with highly-sensitive GECIs revealed that synchronized $[Ca^{2+}]_i$ elevation and its propagation in cell populations occur continuously at the aggregation and mound stages; however, they temporarily disappear during multicellular formation. $Ca^{2+}$ wave propagation depends on cAMP relay at the early aggregation and mound stages, and cAMP wave propagation disappears during tip elongation of the late mound (Fujimori et al., 2019; Hashimura et al., 2019). The cAMP signal has been shown to induce transient $[Ca^{2+}]_i$ elevation (Abe et al., 1988; Nebl and Fisher, 1997). Therefore, changes in the dynamics of $[Ca^{2+}]_i$ during development follow the transition of cAMP relay. Alternatively, we found that $[Ca^{2+}]_i$ burst and its propagation occasionally occurred in slugs. When $[Ca^{2+}]_i$ waves were propagated in the migrating slug, velocity of the slug transiently increased. $Ca^{2+}$ signaling affects both cell movement at the unicellular stage and slug behavior (Dohrmann et al., 1984; Fache et al., 2005; Lombardi et al., 2008). Thus, $[Ca^{2+}]_i$ wave propagation is involved in coordinated movements of multiple cells throughout development. Calcium wave propagation and its effect on cell behavior are also

well known in animal cells, and gap-junction is essential for cell-cell signaling (Leybaert and Sanderson, 2012). Given that *D. discoideum* has no homologue of gap junction components (Johnson et al., 1977; Kaufmann et al., 2012), the mechanism for calcium signal propagation in multicellular bodies is gap junction independent. Another possible mechanism of calcium wave propagation is ATP-mediated paracrine signaling (Leybaert and Sanderson, 2012). It has been reported that *Dictyostelium* cells release ATP as an extracellular signal (Sivaramakrishnan and Fountain, 2015). Extracellular ATP causes an increase in $[Ca^{2+}]_i$ in *Dictyostelium* cells via P2X receptors and polycystin-type Trp channels that are either the ATP receptor or closely coupled to ATP (Ludlow et al., 2008; Traynor and Kay, 2017). Recently, it has been suggested that ATP levels contribute to differentiation during the multicellular phase (Hiraoka et al., 2020). This implies that slug cells secrete ATP, which might trigger wave propagation of elevated $[Ca^{2+}]_i$ in tissue.

*Dictyostelium* cells show $[Ca^{2+}]_i$ elevation in response to cAMP signals and mechanical stimuli at the unicellular phase (Artemenko et al., 2016; Lombardi et al., 2008; Srivastava et al., 2020). Our assay showed that $[Ca^{2+}]_i$ burst and its propagation were induced by mechanical stimuli at the slug stage. The IplA $Ca^{2+}$ channel is involved in $[Ca^{2+}]_i$ elevation in response to mechanical stimuli at the unicellular phase (Artemenko et al., 2016; Lombardi et al., 2008; Srivastava et al., 2020). In slugs of the *iplA*$^-$ strain, the response efficiency of calcium signaling to mechanical stimulation was reduced, suggesting that IplA is responsible for increasing the certainty of response to mechanical stimuli. The IplA channel is

essential for $Ca^{2+}$ dependent flow-directed motility; however, not for chemotactic migration toward cAMP gradients (Lusche et al., 2012). This suggests that the cAMP signaling pathway and the IplA mediated $Ca^{2+}$ signaling pathway affect the downstream independently each other. This proposition is supported by the observation that there is no clear defect in the development of *iplA*$^{-}$ cells under laboratory conditions (Movie 7). However, mechanosensing may play important roles in efficient morphogenesis in natural environments where cells of soil-living amoebae *Dictyostelium* are exposed to various stimuli and physical barriers (Bonner and Lamont, 2005). Therefore, mechanical stimulation response of $Ca^{2+}$ signaling via IplA would be important in natural environments (Movie 2). Alternatively, the calcium signaling response to mechanical stimulation was not completely abolished in *iplA*$^{-}$ slugs, suggesting that other signal pathways are involved in the elevation of cytosolic $[Ca^{2+}]_i$ in the mechanical response of slugs. In higher eukaryotes, the stretch-activated $Ca^{2+}$ permeable ion channel Piezo is involved in mechanical stimulus responses (Coste et al., 2010; Fang et al., 2021). Recently, it has been reported that *D. discoideum* has the homologue of Piezo, PzoA, and disruption of the *pzoA* gene causes the defect of $[Ca^{2+}]_i$ response to mechanical stimuli at the unicellular phase (Srivastava et al., 2020). Additionally, mutant cells lacking PzoA can develop normally under laboratory conditions; however, a defect is observed in chemotactic migration under confined conditions (Srivastava et al., 2020). Slugs with cells lacking *pzoA* did not show a substantial difference in calcium response from the wild type. Notably, the Piezo channel, which works in higher multicellular organisms, works only in the unicellular phase in *Dictyostelium*. Even within *Dictyostelium*, the system changes differently, with

Piezo acting as the main pathway during the unicellular phase, and pathways from the extracellular and ER during the multicellular phase. In IplA-null cells, the $[Ca^{2+}]_i$ response was faster than in the wild type. This indicates that the apparent single-peak $[Ca^{2+}]_i$ burst is a mixture of a fast extracellular $Ca^{2+}$ influx and a slower yet more efficient response from the ER. The delay in the calcium response from the ER compared to extracellular signals may be due to the fact that the signal from mechanoreceptors in the plasma membrane is transmitted via IP3 signaling. Moreover, in the unicellular phase of IplA-null cells, no calcium response to mechanical stimuli was detected, even though IplA is not involved in blebbing, which is regulated by calcium signaling related to mechanical stimulation (Srivastava et al., 2020). In human colorectal carcinoma cell line (DLD1 cells), membrane blebbing is regulated by store-operated calcium entry, which is controlled by ER proteins (Aoki et al., 2021). Alternatively, although no homologue of STIM has been found in *Dictyostelium* (Prakriya and Lewis, 2015), unknown store-operated calcium channels (SOCs) may be transducing mechanical stimuli.

$[Ca^{2+}]_i$ burst at both the tip and posterior regions in slugs indicates the ability of rapid $[Ca^{2+}]_i$ elevation in both prestalk and prespore cells. Previous studies has shown that $[Ca^{2+}]_i$ in the anterior part of the slugs is higher than that in the posterior part (Cubitt et al., 1995; Yumura et al., 1996). However, in our study, such a difference was not observed in slugs at the stationary phase that did not show any $[Ca^{2+}]_i$ burst. As slugs migrate with their tips protruding up and down (Breen et al., 1987), the frequency of $[Ca^{2+}]_i$ bursts evoked by mechanical stimuli

316 is higher in the anterior region that that of the posterior. Thus, it may have been
317 frequently observed in previous studies that $[Ca^{2+}]_i$ is higher in the anterior part
318 of the slug than in the posterior part.
319
320 In conclusion, we revealed that $[Ca^{2+}]_i$ burst and its propagation in populations of
321 *Dictyostelium* cells occur dependently on cell-cell communication via diffusible
322 chemical signals during the early developmental stage. Following multicellular
323 formations, such $Ca^{2+}$ signaling is triggered by mechanical stimuli. The system of
324 $Ca^{2+}$ signaling in response to mechanical stimuli is conserved broadly in higher
325 eukaryotes, animals, and prokaryotes such as *Escherichia coli* (Bruni et al., 2017;
326 Leybaert and Sanderson, 2012; Wakai et al., 2021). We observed that social
327 amoebae *D. discoideum* belonging to Amoebozoa uses $Ca^{2+}$ signaling as a
328 mechanosensing signal at the multicellular phase similarly to the unicellular
329 phase (Srivastava et al., 2020); however, the molecular mechanism is different.
330 Thus, this study demonstrates that mechanochemical signal transduction via
331 $Ca^{2+}$ signaling is a universal system for response to mechanical stimuli and can
332 be applied in any cell type or state. In this study, the extracellular $Ca^{2+}$ pathway
333 associated with mechanical stimulation in the multicellular bodies of *D.*
334 *discoideum* has not been identified. This is because even though $Ca^{2+}$ act as a
335 signal across species, the molecular mechanisms differ between species. Further
336 studies are required to clarify conserved and specific molecular mechanisms,
337 respectively.
338

# Material and Methods

## Cell strains and culture conditions

*Dictyostelium discoideum* strains used in this study are listed in Table S1. The *pzoA*$^{-}$ strain was constructed using the vector pKOSG-IBA-dicty1 (iba) following the manufacturer's instructions (Wiegand et al., 2011). The 5' region and 3' region of flanking sequences were generated via polymerase chain reaction (PCR) and cloned into pKOSG-IBA-dicty1 (Fig. S6A). Primer pairs used for PCR were pzA_KO_LA1/pzA_KO_LA2 (5') and pzA_KO_RA1/pzA_KO_RA2 (3') (Table. S2). *pzoA* gene disruption was confirmed via PCR. Cells were grown axenically in HL5 medium (Formedium, UK) in culture dishes at 21 °C. Transformants were maintained at 20 μg mL$^{-1}$ G418 (Fujifilm Wako, Japan) or 10 μg mL$^{-1}$ BlasticidinS (Fujifilm Wako, Japan).

## Plasmid construction and genetic manipulation

Plasmids used in this study are listed in Table S3. pHK12neo_Dd-GCaMP6s was constructed by insertion of synthesized GCaMP6s fragments (GenScript) into the BglII and SpeI sites of pHK12neo. The codon usages of the GCaMP6s sequence were optimized to those of *D. discoideum* for efficient protein expression in *Dictyostelium* cells. The wild-type strain and mutant cells were transformed with ~1.5 μg plasmid via electroporation (Kuwayama et al., 2008), and transformants were selected with G418 or BlasticidinS.

## Instruments for image acquisition and analysis

In all experiments, cells were observed at 22 °C. Confocal images were taken

363 using a confocal laser microscope (A1 confocal laser microscope system, Nikon,
364 Japan) with an oil immersion lens (Plan Fluor 40×/1.30 NA, Nikon) or an inverted
365 microscope (Eclipse Ti, Nikon) equipped with a CSU-W1 confocal scanner unit
366 (Yokogawa), two sCMOS cameras (ORCA-Flash4.0v3, Hamamatsu Photonics,
367 Japan) and an oil immersion lenses (Plan Apo 60×/1.40 NA or CFI Apo TIRF
368 60×/1.49, Nikon). GCaMP6s and YC-Nano15 were excited using a 488 and 440
369 nm solid-state CW laser, respectively. Epifluorescence imaging was taken using
370 an inverted epifluorescence microscope (IX83, Olympus, Japan) equipped with a
371 130 W mercury lamp system (U-HGLGPS, Olympus), sCMOS cameras (Zyla4.2,
372 Andor Technology or Prime 95B, Photometrics, USA) and objective lenses
373 (UPLSAPO 4×/0.16 NA, UPLSAPO 10×/0.40 NA, UPLSAPO 20×/0.75 NA,
374 Olympus). Cells expressing GCaMP6s were observed using fluorescence mirror
375 units U-FGFP (Excitation BP 460–480, Emission BP 495–540, Olympus). All
376 images were processed and analyzed using Fiji and R software. The period of an
377 oscillation of GCaMP6s signals was calculated by averaging the difference
378 between the peaks of the oscillation. Data with at least three peaks in the
379 oscillation were used for the analysis. In general, fluorescence intensities of
380 GCaMP6s and the ratio of YFP/CFP channels of YCNano15 were normalized
381 with values at t = 0.
382
383 **Live image of $[Ca^{2+}]_i$ dynamics during *Dictyostelium* development**
384 Image acquisition of *Dictyostelium* development was performed as reported by a
385 previous study (Hashimura et al., 2019). To induce development upon starvation,
386 cells at the exponential phase (1.5–3 × $10^6$ cells $ml^{-1}$) were harvested and

washed three times in KK2 phosphate buffer (20 mM $KH_2PO_4/K_2HPO_4$, pH 6.0). To observe all developmental stages, cells were plated on the entire surface of 2% water agar (2% w/v Difco Bacto-agar in ultrapure water) at a density of 5–7 × $10^5$ cells $cm^{-2}$ on a 35-mm plastic dish (Iwaki, Japan) and incubated at 21 °C. Thereafter, plates were filled with liquid paraffin (Nacalai Tesque, Japan) to avoid light scattering and placed on the stage of the microscope for image acquisition. Additionally, the "2D slug" method (Bonner, 1998; Rieu, Barentin, Sawai, Maeda, & Sawada, 2004) was applied for observing slug migration without three-dimensional scroll movement (Fig. 4A and S2). One microliter cell suspension (4 × $10^7$ cells $mL^{-1}$) was dropped on 2% water agar plates with 2 µL liquid paraffin. A coverslip was placed over the suspension and incubated at 21 °C for longer than 15 h.

**Validation of GCaMP6s as an indicator of $[Ca^{2+}]_i$ changes in chemotactic-competent *Dictyotelium* cells**

*Dictyostelium* cells expressing Dd-GCaMP6s were suspended in 1 mL developmental buffer (DB: 5 mM $Na/KPO_4$, 2 mM $MgSO_4$, 0.2 mM $CaCl_2$, pH 6.5) at a density of 5 × $10^5$ cells $mL^{-1}$ and incubated for 1 h. Thereafter, cells were exposed to 100 nM cAMP pulses given at 6 min intervals for a subsequent 5 h. Following starvation with cAMP pulse treatment, cells were washed three times with 1 mL DB and resuspended in DB at a density of $10^6$ cells $mL^{-1}$. Forty microliters of cell suspension was deposited onto a glass bottom dish. Cells were stimulated by adding 160 µL of 12.5 µM cAMP (Sigma Aldrich, USA) solution to the cell droplet (final concentration, 10 µM). During stimulation, fluorescent

411 images of starved cells were taken using the confocal microscope at 5 s interval.
412 Averaged fluorescence intensities of GCaMP6s in 5 $\mu m^2$ regions positioned within
413 the cytosol were estimated at each time point.
414
415 **Monitoring of $[Ca^{2+}]_i$ response in slugs to mechanical stimulation**
416 To observe the response of migrating slugs to mechanical stimulation, 5 µL of cell
417 suspension at a density of $4 \times 10^7$ cells $mL^{-1}$ was deposited on 2% water agar
418 with or without 1 mM EGTA and incubated at 21 °C for 12–15 h. Following slug
419 formation, a piece of agar with slugs was cut out and placed upside down on a
420 spacer attached to a 35 mm glass bottom dish (12 mm diameter glass, Iwaki).
421 The spacer was filled with liquid paraffin to prevent desiccation during observation
422 and avoid light scattering. A slug covered by agar was pushed with a 5 mm
423 diameter plastic rod using a micromanipulator system (MM-94 and MMO-4,
424 Narishige, Japan) (Fig. S4A). In the micropipette assay, a piece of agar with slugs
425 was cut out and placed directly on a 35 mm glass bottom dish (12 mm diameter
426 glass, Iwaki). A wet paper was placed in the dish and the agar piece was covered
427 with liquid paraffin. A Femtotip microcapillary (1 µm tip diameter, Eppendorf,
428 Germany) was mounted onto a Femtojet pump and micromanipulator
429 (Eppendorf), and the pipette was pricked on the slug by manual operation with
430 the manipulator (Fig. S4B). During mechanical stimulation, fluorescence images
431 of slugs expressing GCaMP6s were acquired at 5 s interval using the
432 epifluorescence microscope.
433
434
435

## Acknowledgements

We acknowledge Yuko Baba for technical assistance and Takuo Yasunaga for continuous support and encouragement. H.H. was supported by the RIKEN JRA program.

## Competing interests

The authors declare no competing interests.

## Author contributions

H.H. conceived and designed the study, performed the experiments, analyzed the data, and wrote the manuscript. Y.H. performed the experiments and analyzed the data. M.U. designed the study, contributed to the interpretation of the data analysis. Y.V.M. designed the study, performed the experiments, analyzed the data and wrote the manuscript.

## Funding

This work was supported in part by JSPS KAKENHI Grant Numbers JP19H00982 (to M.U.), JP15H05593, JP18K06159 and JP21K06099 (to Y.V.M.), JP20J00751 and JP21K15081 (to H.H.) and JST PRESTO Grant Number JPMJPR204B (to Y.V.M.). This work has also been partially supported by AMED-CREST Grant Number JP20gm0910001.

## References

**Abe, T., Maeda, Y. and Iijima, T.** (1988). Transient increase of the intracellular $Ca^{2+}$ concentration during chemotactic signal transduction in *Dictyostelium discoideum* cells. *Differentiation* **39**, 90-96.

**Aoki, K., Harada, S., Kawaji, K., Matsuzawa, K., Uchida, S. and Ikenouchi, J.** (2021). STIM-Orai1 signaling regulates fluidity of cytoplasm during membrane blebbing. *Nat Commun* **12**, 480.

**Artemenko, Y., Axiotakis, L., Jr., Borleis, J., Iglesias, P. A. and Devreotes, P. N.** (2016). Chemical and mechanical stimuli act on common signal transduction and cytoskeletal networks. *Proc Natl Acad Sci U S A* **113**, E7500-E7509.

**Berridge, M. J., Bootman, M. D. and Roderick, H. L.** (2003). Calcium signalling: dynamics, homeostasis and remodelling. *Nat Rev Mol Cell Biol* **4**, 517-529.

**Bonner, J. T. and Lamont, D. S.** (2005). Behavior of cellular slime molds in the soil. *Mycologia* **97**, 178-184.

**Breen, E. J., Vardy, P. H. and Williams, K. L.** (1987). Movement of the multicellular slug stage of *Dictyostelium discoideum*: an analytical approach. *Development* **101**, 313.

**Bruni, G. N., Weekley, R. A., Dodd, B. J. T. and Kralj, J. M.** (2017). Voltage-gated calcium flux mediates *Escherichia coli* mechanosensation. *Proc Natl Acad Sci U S A* **114**, 9445-9450.

**Canales, J., Morales, D., Blanco, C., Rivas, J., Diaz, N., Angelopoulos, I. and Cerda, O.** (2019). A TR(i)P to Cell Migration: New Roles of TRP Channels in Mechanotransduction and Cancer. *Front Physiol* **10**, 757.

**Chen, T. W., Wardill, T. J., Sun, Y., Pulver, S. R., Renninger, S. L., Baohan, A., Schreiter, E. R., Kerr, R. A., Orger, M. B., Jayaraman, V., et al.** (2013). Ultrasensitive fluorescent proteins for imaging neuronal activity. *Nature* **499**, 295-300.

**Chifflet, S., Justet, C., Hernandez, J. A., Nin, V., Escande, C. and Benech, J. C.** (2012). Early and late calcium waves during wound healing in corneal endothelial cells. *Wound Repair Regen* **20**, 28-37.

**Clapham, D. E.** (2007). Calcium signaling. *Cell* **131**, 1047-1058.

**Coste, B., Mathur, J., Schmidt, M., Earley, T. J., Ranade, S., Petrus, M. J., Dubin, A. E. and Patapoutian, A.** (2010). Piezo1 and Piezo2 are essential components of distinct mechanically activated cation channels.

*Science* **330**, 55-60.

**Cubitt, A. B., Firtel, R. A., Fischer, G., Jaffe, L. F. and Miller, A. L.** (1995). Patterns of free calcium in multicellular stages of *Dictyostelium* expressing jellyfish apoaequorin. *Development* **121**, 2291-2301.

**Dohrmann, U., Fisher, P. R., Bruderlein, M. and Williams, K. L.** (1984). Transitions in *Dictyostelium discoideum* behaviour: influence of calcium and fluoride on slug phototaxis and thermotaxis. *J Cell Sci* **65**, 111-121.

**Fache, S., Dalous, J., Engelund, M., Hansen, C., Chamaraux, F., Fourcade, B., Satre, M., Devreotes, P. and Bruckert, F.** (2005). Calcium mobilization stimulates *Dictyostelium discoideum* shear-flow-induced cell motility. *J Cell Sci* **118**, 3445-3457.

**Fang, X. Z., Zhou, T., Xu, J. Q., Wang, Y. X., Sun, M. M., He, Y. J., Pan, S. W., Xiong, W., Peng, Z. K., Gao, X. H., et al.** (2021). Structure, kinetic properties and biological function of mechanosensitive Piezo channels. *Cell Biosci* **11**, 13.

**Fujimori, T., Nakajima, A., Shimada, N. and Sawai, S.** (2019). Tissue self-organization based on collective cell migration by contact activation of locomotion and chemotaxis. *Proc Natl Acad Sci U S A* **116**, 4291-4296.

**Gregor, T., Fujimoto, K., Masaki, N. and Sawai, S.** (2010). The onset of collective behavior in social amoebae. *Science* **328**, 1021-1025.

**Hashimura, H., Morimoto, Y. V., Yasui, M. and Ueda, M.** (2019). Collective cell migration of *Dictyostelium* without cAMP oscillations at multicellular stages. *Commun Biol* **2**, 34.

**Hiraoka, H., Nakano, T., Kuwana, S., Fukuzawa, M., Hirano, Y., Ueda, M., Haraguchi, T. and Hiraoka, Y.** (2020). Intracellular ATP levels influence cell fates in *Dictyostelium discoideum* differentiation. *Genes Cells* **25**, 312-326.

**Horikawa, K., Yamada, Y., Matsuda, T., Kobayashi, K., Hashimoto, M., Matsu-ura, T., Miyawaki, A., Michikawa, T., Mikoshiba, K. and Nagai, T.** (2010). Spontaneous network activity visualized by ultrasensitive $Ca^{2+}$ indicators, yellow Cameleon-Nano. *Nat Methods* **7**, 729-732.

**Johnson, G., Johnson, R., Miller, M., Borysenko, J. and Revel, J. P.** (1977). Do cellular slime molds form intercellular junctions? *Science* **197**, 1300.

**Kaufmann, S., Weiss, I. M., Eckstein, V. and Tanaka, M.** (2012). Functional expression of $Ca^{2+}$ dependent mammalian transmembrane gap junction protein Cx43 in slime mold *Dictyostelium discoideum*. *Biochem Biophys*

*Res Commun* **419**, 165-169.

**Kuwayama, H., Yanagida, T. and Ueda, M.** (2008). DNA oligonucleotide-assisted genetic manipulation increases transformation and homologous recombination efficiencies: Evidence from gene targeting of *Dictyostelium discoideum*. *J Biotechnol* **133**, 418-423.

**Leybaert, L. and Sanderson, M. J.** (2012). Intercellular $Ca^{2+}$ waves: mechanisms and function. *Physiol Rev* **92**, 1359-1392.

**Lombardi, M. L., Knecht, D. A. and Lee, J.** (2008). Mechano-chemical signaling maintains the rapid movement of *Dictyostelium* cells. *Exp Cell Res* **314**, 1850-1859.

**Ludlow, M. J., Traynor, D., Fisher, P. R. and Ennion, S. J.** (2008). Purinergic-mediated $Ca^{2+}$ influx in *Dictyostelium discoideum*. *Cell Calcium* **44**, 567-579.

**Lusche, D. F., Wessels, D., Scherer, A., Daniels, K., Kuhl, S. and Soll, D. R.** (2012). The IplA $Ca^{2+}$ channel of *Dictyostelium discoideum* is necessary for chemotaxis mediated through $Ca^{2+}$, but not through cAMP, and has a fundamental role in natural aggregation. *J Cell Sci* **125**, 1770-1783.

**Nebl, T. and Fisher, P. R.** (1997). Intracellular $Ca^{2+}$ signals in *Dictyostelium* chemotaxis are mediated exclusively by $Ca^{2+}$ influx. *J Cell Sci* **110 ( Pt 22)**, 2845-2853.

**Parekh, A. B.** (2011). Decoding cytosolic $Ca^{2+}$ oscillations. *Trends Biochem Sci* **36**, 78-87.

**Pervin, M. S., Itoh, G., Talukder, M. S. U., Fujimoto, K., Morimoto, Y. V., Tanaka, M., Ueda, M. and Yumura, S.** (2018). A study of wound repair in *Dictyostelium* cells by using novel laserporation. *Sci Rep* **8**, 7969.

**Prakriya, M. and Lewis, R. S.** (2015). Store-Operated Calcium Channels. *Physiol Rev* **95**, 1383-1436.

**Prole, D. L. and Taylor, C. W.** (2019). Structure and Function of IP3 Receptors. *Cold Spring Harb Perspect Biol* **11**.

**Schlatterer, C., Knoll, G. and Malchow, D.** (1992). Intracellular calcium during chemotaxis of *Dictyostelium discoideum*: a new fura-2 derivative avoids sequestration of the indicator and allows long-term calcium measurements. *Eur J Cell Biol* **58**, 172-181.

**Singer, G., Araki, T. and Weijer, C. J.** (2019). Oscillatory cAMP cell-cell signalling persists during multicellular *Dictyostelium* development. *Commun Biol* **2**, 139.

**Sivaramakrishnan, V. and Fountain, S. J.** (2015). Evidence for Extracellular ATP as a Stress Signal in a Single-Celled Organism. *Eukaryot Cell* **14**, 775-782.

**Srivastava, N., Traynor, D., Piel, M., Kabla, A. J. and Kay, R. R.** (2020). Pressure sensing through Piezo channels controls whether cells migrate with blebs or pseudopods. *Proc Natl Acad Sci U S A* **117**, 2506-2512.

**Tomchik, K. J. and Devreotes, P. N.** (1981). Adenosine 3',5'-monophosphate waves in *Dictyostelium discoideum*: a demonstration by isotope dilution--fluorography. *Science* **212**, 443-446.

**Traynor, D. and Kay, R. R.** (2017). A polycystin-type transient receptor potential (Trp) channel that is activated by ATP. *Biol Open* **6**, 200-209.

**Traynor, D., Milne, J. L., Insall, R. H. and Kay, R. R.** (2000). $Ca^{2+}$ signalling is not required for chemotaxis in *Dictyostelium*. *EMBO J* **19**, 4846-4854.

**Volkers, L., Mechioukhi, Y. and Coste, B.** (2015). Piezo channels: from structure to function. *Pflugers Arch* **467**, 95-99.

**Wakai, M. K., Nakamura, M. J., Sawai, S., Hotta, K. and Oka, K.** (2021). Two-Round $Ca^{2+}$ transient in papillae by mechanical stimulation induces metamorphosis in the ascidian Ciona intestinalis type A. *Proc Biol Sci* **288**, 20203207.

**Weijer, C. J.** (1999). Morphogenetic cell movement in *Dictyostelium*. *Semin Cell Dev Biol* **10**, 609-619.

**Whitaker, M.** (2006). Calcium at fertilization and in early development. *Physiol Rev* **86**, 25-88.

**Wiegand, S., Kruse, J., Gronemann, S. and Hammann, C.** (2011). Efficient generation of gene knockout plasmids for *Dictyostelium discoideum* using one-step cloning. *Genomics* **97**, 321-325.

**Yin, J. and Kuebler, W. M.** (2010). Mechanotransduction by TRP channels: general concepts and specific role in the vasculature. *Cell Biochem Biophys* **56**, 1-18.

**Yumura, S., Furuya, K. and Takeuchi, I.** (1996). Intracellular free calcium responses during chemotaxis of *Dictyostelium* cells. *J Cell Sci* **109 ( Pt 11)**, 2673-2678.

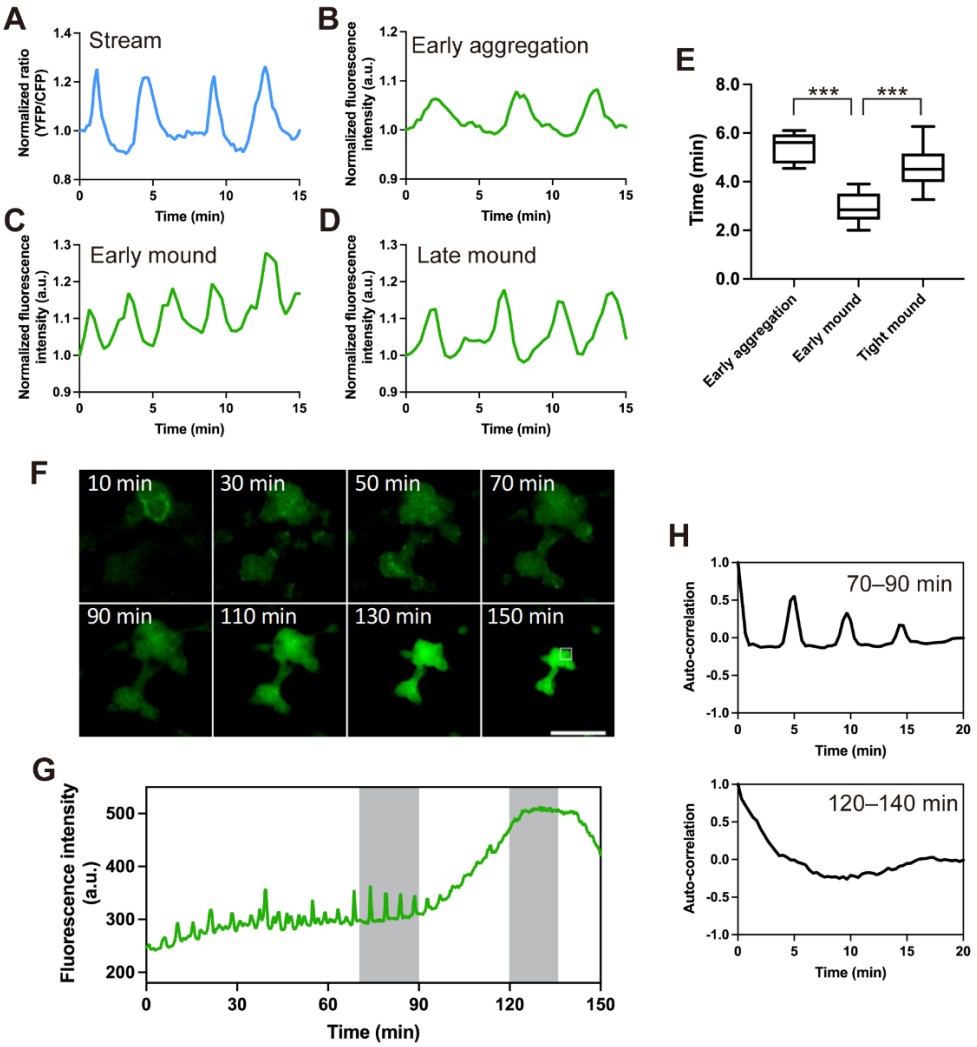


**Fig. 1. $[Ca^{2+}]_i$ signal dynamics at each developmental stage of *Dictyostelium* cells.** Time course plots of (A) Förster resonance energy transfer (FRET) signals of YC-Nano15 or (B–D) mean fluorescence intensity of GCaMP6s in a region indicated by a white box (ROI) in Fig. S1. Size of ROI: A, 25 μm. B, 250 μm. C and D, 100 μm. (A) An aggregating stream. (B) Early aggregation. (C) An early mound. (D) A late mound. (E) Boxplot of periods of $[Ca^{2+}]_i$ oscillations at three developmental stages. The lower and upper error lines indicate the smallest and largest values, respectively. At each dataset, n = 13. ***; $p < 0.001$ (Wilcoxon rank sum test). (F) Fluorescence images of *Dictyostelium* cells expressing GCaMP6s during morphogenesis from the late mound to the finger stage. Scale bar, 500 μm. (G) Time course plot of mean fluorescence intensity of GCaMP6s in a 100 $\mu m^2$ region indicated by a white box in F. (H) Autocorrelation of GCaMP6s signals at each development stage shown by gray bars in G. Note that the elevation of fluorescence intensity in the entire mound (90–150 min in F and G) is primarily due to the increase in thickness of the tissue rather than $[Ca^{2+}]_i$ elevation.

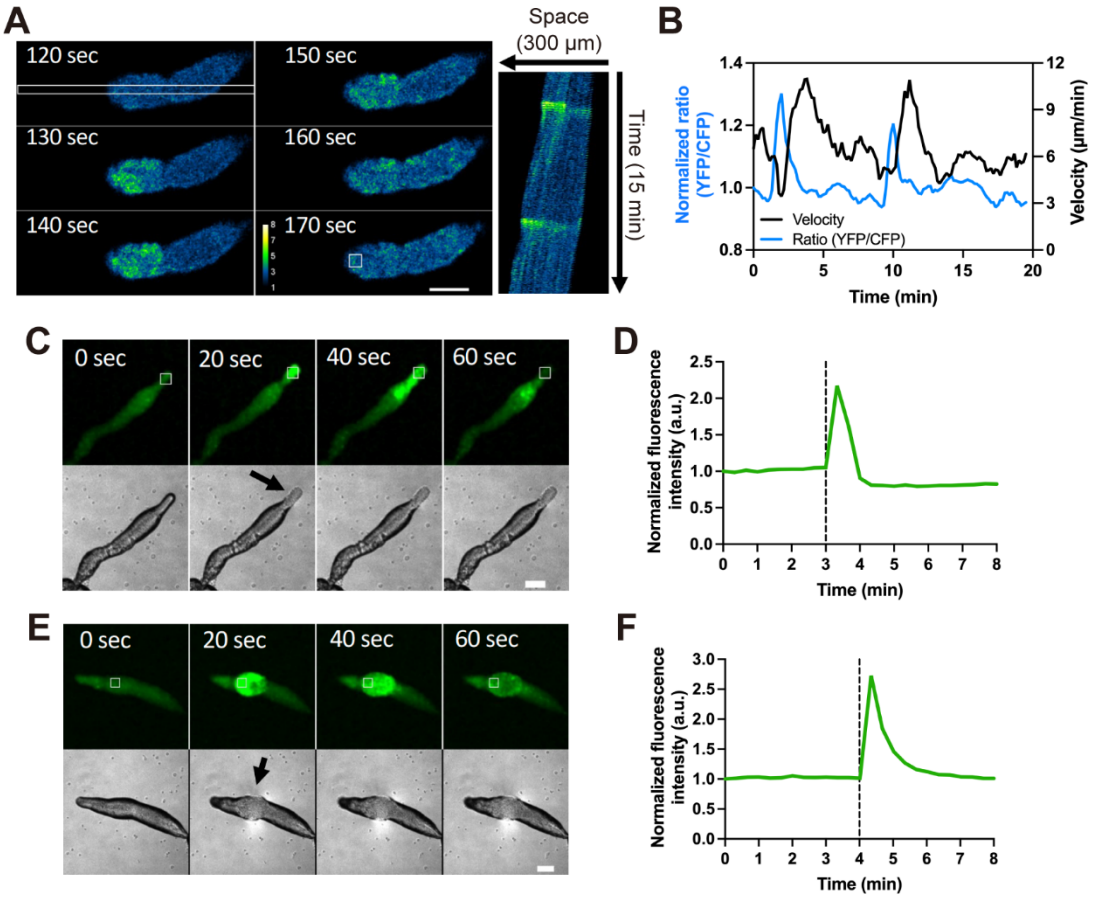


**Fig. 2. Intracellular $Ca^{2+}$ levels ($[Ca^{2+}]_i$) burst in *Dictyostelium* slugs during migration.** (A) Ratiometric images (YFP/CFP) of a slug expressing YC-Nano15 (Left). $[Ca^{2+}]_i$ burst at a tip of the slug expressing YC-Nano15 and its propagation toward the posterior region of the slug are shown. Scale bar, 50 μm. (Right) The kymograph of $[Ca^{2+}]_i$ wave propagation in the region indicated by a white rectangle (10×300μm) in the left panel for 15 min duration. (B) Time-course plot of Förster resonance energy transfer (FRET) signals in the tip of the slug (blue line) and slug velocity (black line). The FRET signals of YC-Nano15 in a 15 $\mu m^2$ region in the slug (white box in A) was measured. The curves of FRET signals and slug velocity were smoothed by a running average over four data points. (C and E) $[Ca^{2+}]_i$ burst at a tip (C) or posterior region (E) of the slug expressing GCaMP6s. Fluorescence images of GCaMP6s (upper panels)and differential interference contrast (DIC) images (lower panels) are shown. Scale bar, 100 μm. An arrow shows that the slugs are in contact with the agar surface. (D and F) Time course plot of the mean fluorescence intensity of GCaMP6s in a 50 $\mu m^2$ region indicated by a white box in C and E. Black dashed lines indicate the time point when the slug was in contact with the agar surface.

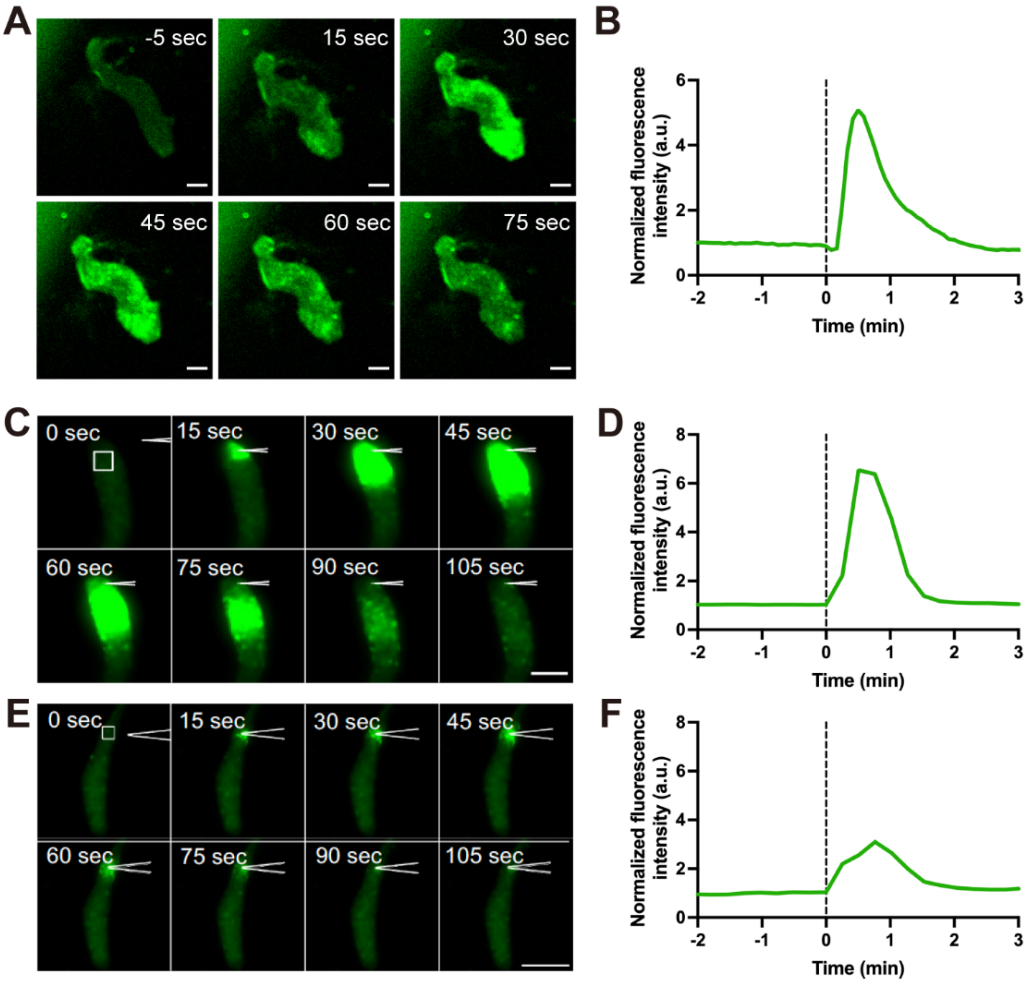


**Fig. 3. Intracellular $Ca^{2+}$ levels ($[Ca^{2+}]_i$) burst in *Dictyostelium* slugs induced by mechanical stimulation.** (A) Representative fluorescence images of a slug expressing GCaMP6s mechanically stimulated with a plastic rod. Scale bar, 50 μm. (B) Time course plot of the mean fluorescence intensity of GCaMP6s in a 25 $\mu m^2$ ROI of the anterior region in A. (C and E) $[Ca^{2+}]_i$ burst at the tip (C) or posterior region (E) of the slug expressing Dd-GCaMP6s after mechanical stimulation by pricking with a micropipette. Fluorescence images of slugs expressing Dd-GCaMP6s are shown. Anterior part of the slug faces the top (C) or bottom (E) side of images. Scale bar, (C) 50 and (E) 100 μm. (D and F) Time course plot of the mean fluorescence intensity of GCaMP6s in a 25 $\mu m^2$ region indicated by a white box in C and E, respectively. Black dashed lines indicate the time point of mechanical stimulation.

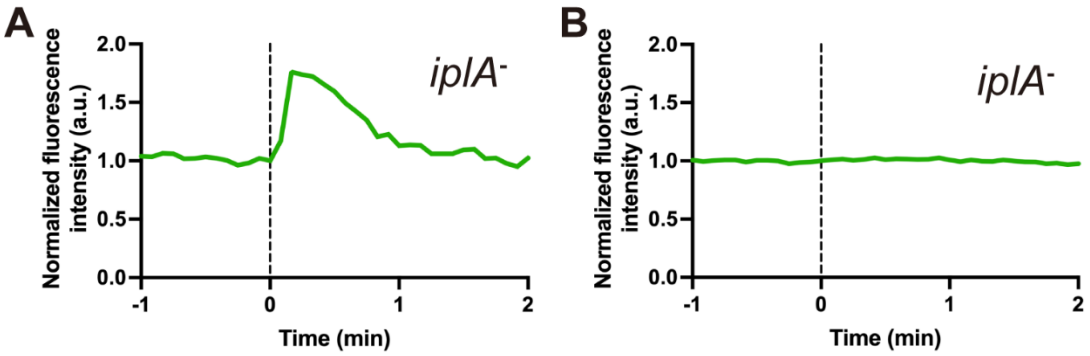


**Fig. 4. Intracellular $Ca^{2+}$ levels ($[Ca^{2+}]_i$) burst in *iplA*$^-$ slugs induced by mechanical stimulation.** $[Ca^{2+}]_i$ was monitored in the slug of IplA null cells expressing GCaMP6s after mechanical stimulation with a plastic rod. (A) Representative time course plot of the mean fluorescence intensity of GCaMP6s in a slug showing $[Ca^{2+}]_i$ burst. (B) Representative time course plot of the mean fluorescence intensity of GCaMP6s in a slug showing no $[Ca^{2+}]_i$ response. Black dashed lines indicate the time point of mechanical stimulation.

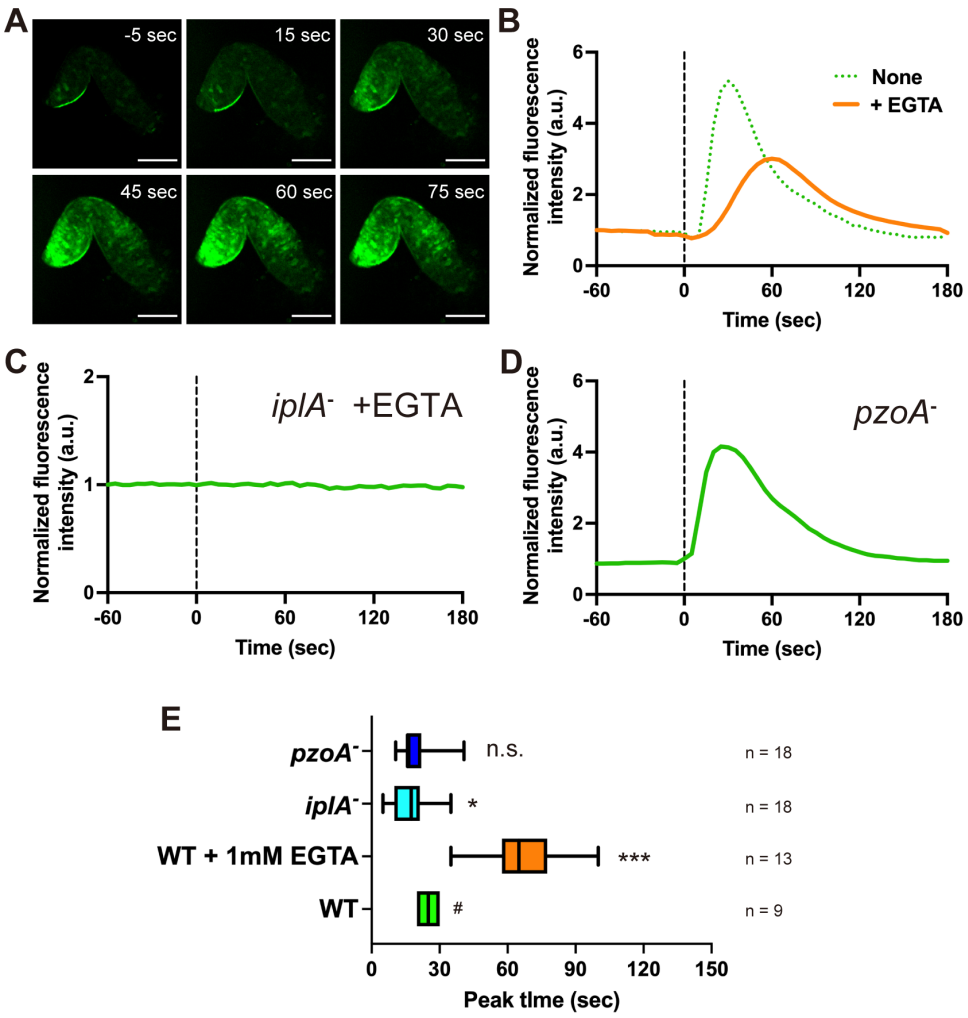


**Fig. 5. Effect of extracellular $Ca^{2+}$ on intracellular $Ca^{2+}$ levels ($[Ca^{2+}]_i$) burst in *Dictyostelium* slugs induced by mechanical stimulation.** (A) A wild-type slug was covered with a piece of agar containing 1 mM aminoethyl ether)-N,N,N′ ,N′ -tetraacetic acid (EGTA). Representative fluorescence images of GCaMP6s in a slug mechanically stimulated with a rod on EGTA agar. Scale bar, 100 μm. (B) Orange line shows time course plot of the mean fluorescence intensity of GCaMP6s in a 25 $\mu m^2$ ROI of the anterior region in A. The green dashed line shows the plot of fluorescence intensity without EGTA in Fig. 3B. (C) Time course plot of the mean fluorescence intensity of GCaMP6s in the slug of IplA null cells with agar containing 1 mM EGTA. (D) Time course plot of the mean fluorescence intensity of GCaMP6s in the slug of PzoA null cells without 1 mM EGTA. (E) Box plots of the peak time of $[Ca^{2+}]_i$ burst after mechanical stimuli. Lower and upper error lines indicate the smallest and largest values, respectively. Average values were compared with the peak time of the wild-type slug without EGTA (#). *, $p < 0.05$; ***; $p < 0.001$ (Two tailed *t*-test). n.s. indicates no significant difference.